



Trade Science Inc.

# Nano Science and Nano Technology

*An Indian Journal*


---

**Full Paper**

NSNTAJ, 7(2), 2013 [73-78]

## Immobilization of Ni nanoparticles on micron aluminum and the corrosion characteristics of the Al/Ni bimetallic nanocomposite

Yi Wang\*, Wei Jiang, Hongying Liu, Fengsheng Li

National Special Superfine Powder Engineering Research Center, Nanjing University of Science and Technology, Nanjing 210094, (CHINA)

Received: 13<sup>th</sup> August, 2012 ; Accepted: 12<sup>th</sup> September, 2012

### ABSTRACT

The displacement method was employed to modify the surface of micron Al on which a layer of Ni nanoparticles were coated.  $\text{NH}_4\text{F}$  acted as a key that enabled the displacement reaction occurring in neutral solution. PEG600 prevented Al from being corroded by water and restricted the overgrowth of Ni nanoparticles. Other parameters, such as  $\text{NH}_4\text{F}$  and  $\text{NiCl}_2 \cdot 6\text{H}_2\text{O}$  concentrations, were determined by experiment and discussion to be  $0.2 \text{ mol} \cdot \text{L}^{-1}$  and  $1.17 \text{ g} \cdot \text{L}^{-1}$ , respectively. The fabricated Al/Ni bimetallic nanocomposites were corroded by hydrochloric acid solution and alkaline NaOH solution to investigate its corrosion characteristics. After being etched by the acidic solution, micron Al cores were eroded and Ni shells remained. However, the Ni shells broke into fragments after the Al cores were dissolved in the alkaline solution.

© 2013 Trade Science Inc. - INDIA

### KEYWORDS

Nanocomposites;  
Core-shell structure;  
Displacement method;  
Al powder;  
Corrosion.

### INTRODUCTION

Modification of micron granules by nanoparticles, i.e. fabrication of core-shell nanocomposites, combines both the advantages of micron cores and nano shells<sup>[1-3]</sup>. These new materials exhibit different characteristics to their cores and shells<sup>[4-7]</sup>. Micron Al particles are used as the fuel in solid propellants or aluminized explosives<sup>[8-10]</sup>. Usually, these metallic particles were oxidized by air firstly and produced dense layers capping available Al. This blocks the further oxidation of Al particles. Thermal analysis indicates that the ignition point of micron Al is more than  $2100 \text{ }^\circ\text{C}$ <sup>[11,12]</sup>. Therefore, if the alumina layers are replaced by layers of metallic nanoparticles, the reactivity of micron Al will be remark-

ably enhanced.

Some studies reported the fabrication of Al-based nanocomposites by using electroless plating<sup>[13-16]</sup>. Xiong et al. studied the mechanism of electroless plating and established the kinetic model for the deposition of Ni on micron Al<sup>[17,18]</sup>. However, these studies showed that the solutions for plating have high pH values; it is easy to erode available Al cores. Therefore, a lowly corrosive medium becomes the requirement to prepare Al-based nanocomposites. As the alternative, displacement method is more proper to deposit metal nanoparticles on micron Al. The displacement method is also a type of electroless plating, where the reducing agent is the metallic core itself. Compared to conventional electroless plating, the displacement method is superior in de-

## Full Paper

positing nanoparticles in situ. Other characteristics of the displacement method are also attractive to researchers, including its simplicity, its high reaction speed, and low impurity. Using displacement method, Mou et al. prepared Sn/Cu composites with metallic Cu and Sn as the core and shell<sup>[19]</sup>. Liu et al. coated the Cu particles with Ag nanoparticles<sup>[20]</sup>. Using redox reaction between metallic Cu and  $[\text{Ag}(\text{NH}_3)_2]\text{OH}\cdot x\text{H}_2\text{O}$ , Gao introduced Cu particles into a silver-ammonia solution to fabricate Cu/Ag composites<sup>[21]</sup>. A potential advantage of Al-based core-shell composites is that the Al core can be removed. This paper described how the Al/Ni nanocomposites were fabricated and whether the shells subjected to the etching process could be retained.

### EXPERIMENTAL

The displacement reaction between  $\text{Ni}^{2+}$  ions and metallic Al occurred since a 1.414 V potential difference

existed between  $\varphi^0(\text{Al}^{3+}/\text{Al})$  (-1.66V) and  $\varphi^0(\text{Ni}^{2+}/\text{Ni})$  (-0.246 V). The surfactant was introduced to  $\text{NiCl}_2\cdot 6\text{H}_2\text{O}$  aqueous solution. Raw Al were added into the above solution and the  $\text{NH}_4\text{F}$  solution was introduced into (to remove the  $\text{Al}_2\text{O}_3$  layers). The reaction ceased when the suspension was unable to change the color of the SDT, and the product was separated. After filtration, lavation and evaporation in vacuum at 40°C, the Al/Ni core-shell nanocomposites were fabricated. The as-prepared Al/Ni nanocomposites were

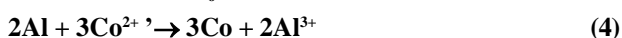
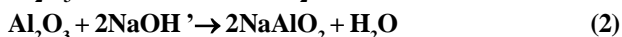
added into acidic or alkaline solutions to remove the Al core for further investigation.

The morphology of the samples was examined by a LEO-1530VP field-emission scanning electron microscope (SEM). X-ray powder diffraction (XRD) analysis was conducted on a Bruker Advance D8 Diffractometer operated at 40 kV and 35mA using Cu K $\alpha$  radiation.

### RESULT AND DISCUSSION

#### Initiation of displacement reaction

During fabrication,  $\text{NH}_4\text{F}$  acted as a key to incur a displacement reaction. Usually, Al particles were coated with dense  $\text{Al}_2\text{O}_3$  layers (amorphous) that restricted the further oxidation of element Al by air, water, even  $\text{Ni}^{2+}$  ions in preparation. Due to the especial property of  $\text{Al}_2\text{O}_3$ , most strong acids and alkalis could dissolve it (Eqs. 1 and 2)<sup>[22]</sup>:



However, having dissolved alumina layers, the acids and alkalis will further erode the available Al. Therefore, it is necessary to give more prominence on the method of properly removing alumina layers. It is reported that F<sup>-</sup> anion can irreversibly react with alumina (Eq. 3), for which the reaction (Eq. 1) was accelerated in the absence of strong acids<sup>[23]</sup>. After the  $\text{Al}_2\text{O}_3$  layers were removed, the “candidate reaction”, i.e. the displace-

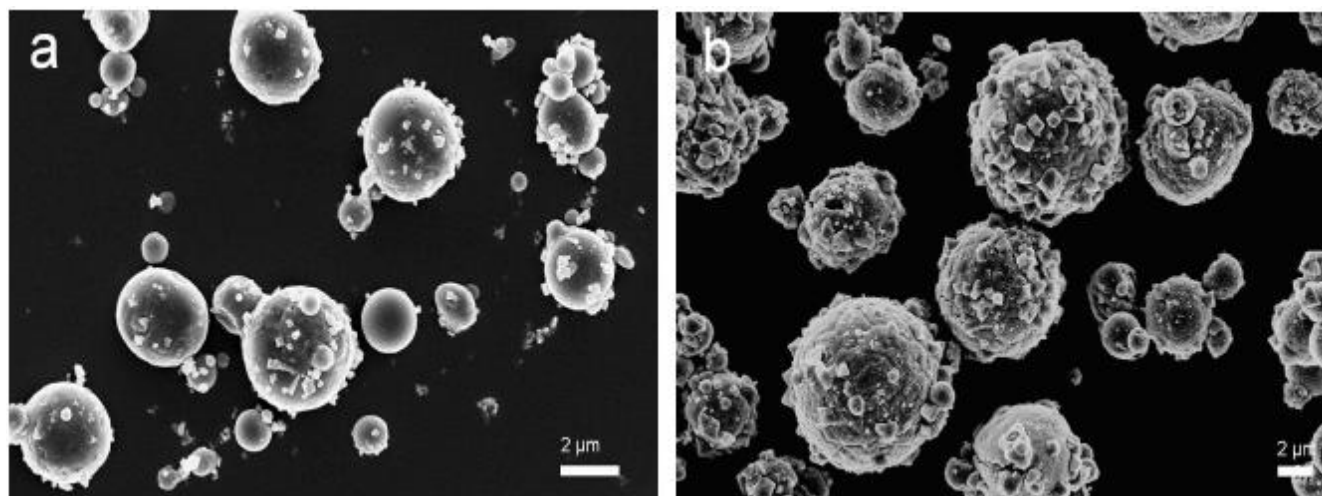


Figure 1 : SEM images of raw Al (a) and (b) Al/Ni prepared with OP as surfactant.

ment reaction between metallic Al and  $\text{Co}^{2+}$  ions (Eq. 4), occurred.

During fabrication, a surfactant was necessary to limiting the overgrowth of displaced Ni particles and to preventing Al cores from being eroded by the solution. In our study, we tried using OP, sodium oleate, and PEG600 as the surfactant. The experimental results showed that OP was not able to protect element Al because many bubbles were observed during the reaction. Figure 1(b) illustrates some of the Al particle erosion. The use of sodium oleate resulted in the serious aggregation of Al particles. Al/Ni nanocomposites were successfully fabricated by using PEG600 as surfactant.

### Ammonium fluoride and precursor concentration

Systems with four  $\text{NH}_4\text{F}$  concentrations ( $0.08 \text{ mol}\cdot\text{L}^{-1}$ ,  $0.14 \text{ mol}\cdot\text{L}^{-1}$ ,  $0.2 \text{ mol}\cdot\text{L}^{-1}$ , and  $0.32 \text{ mol}\cdot\text{L}^{-1}$ ) were studied and the products are shown in Figure 2. At less than  $0.1 \text{ mol}\cdot\text{L}^{-1}$ , few tiny particles were deposited on Al surface (Figure.2b). When the concentration increased to  $0.14 \text{ mol}\cdot\text{L}^{-1}$ , Al cores were ornamented by many small particles (Figure.2c). At  $0.2 \text{ mol}\cdot\text{L}^{-1}$ , layers of nano particles densely coated on the cores (Figure.2d and e). At the concentration of  $0.32 \text{ mol}\cdot\text{L}^{-1}$ , the Al cores were obviously eroded and the etched particles are illustrated in Figure.2f. Therefore, the proper concentration of  $\text{NH}_4\text{F}$  was  $0.2 \text{ mol}\cdot\text{L}^{-1}$ .

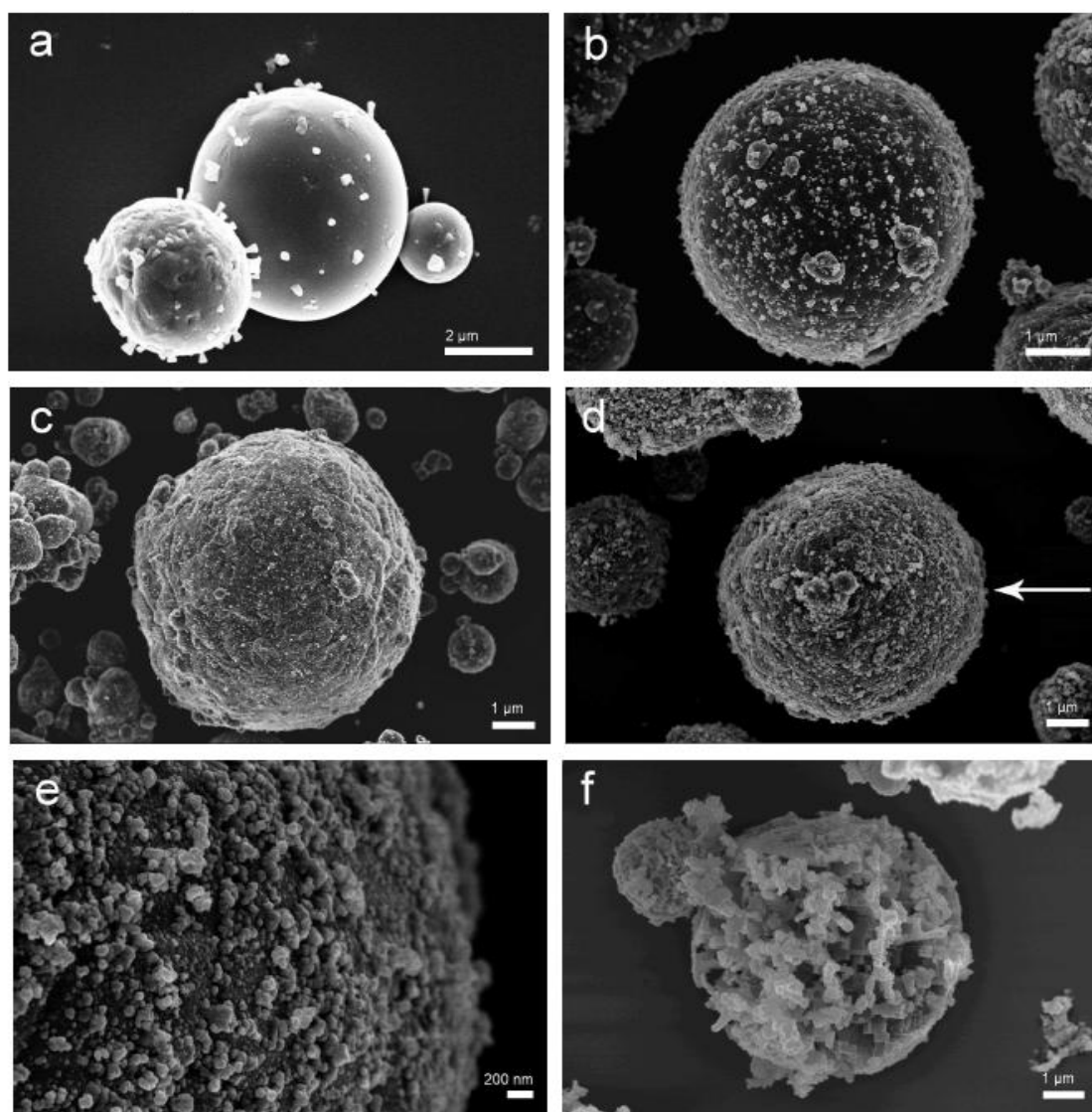
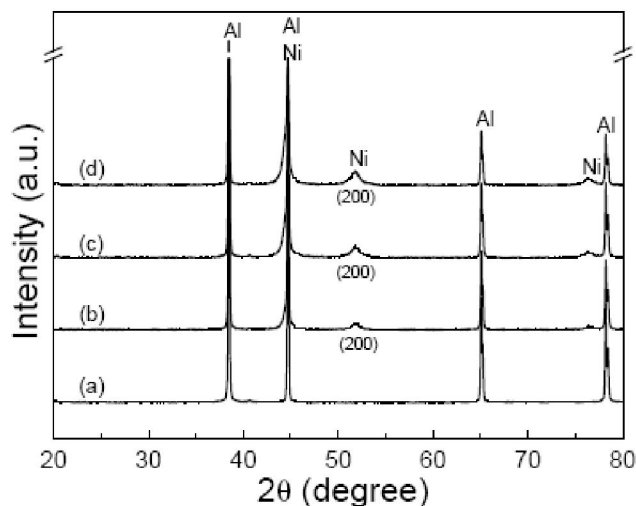


Figure 2 : SEM images of Al/Ni prepared at different  $\text{NH}_4\text{F}$  concentrations: (a) raw Al; (b) concentration of  $0.08 \text{ mol}\cdot\text{L}^{-1}$ ; (c) concentration of  $0.14 \text{ mol}\cdot\text{L}^{-1}$ ; (d) concentration of  $0.2 \text{ mol}\cdot\text{L}^{-1}$ ; (e) partial surface of the particle pointed with an arrow shown in Figure 3d; (f) concentration of  $0.32 \text{ mol}\cdot\text{L}^{-1}$ .

## Full Paper

Besides, the precursor concentration, which determines the reaction rate, is also important. In this case, the weight percentage of Ni (in Al/Ni) and concentration of  $\text{NH}_4\text{F}$  were kept at approximately 3.0 wt.% and  $0.2 \text{ mol}\cdot\text{L}^{-1}$ , respectively. Concentrations of  $\text{NiCl}_2\cdot 6\text{H}_2\text{O}$  were  $2.34 \text{ g}\cdot\text{L}^{-1}$ ,  $1.17 \text{ g}\cdot\text{L}^{-1}$ , and  $0.78 \text{ g}\cdot\text{L}^{-1}$ . The XRD patterns of the products are shown in Figure 3. By compared the pattern of raw Al, the diffraction peaks of metallic Ni exist (in Figure 3b-d). The peaks at  $2\theta$  of  $38.47^\circ$ ,  $44.90^\circ$ ,  $65.09^\circ$ , and  $78.22^\circ$  belonged to the {111}, {200}, {220}, and {311} planes of Al; the peaks at  $2\theta$  of  $44.79^\circ$ ,  $51.85^\circ$ , and  $76.38^\circ$  corresponded to the {111}, {200}, and {220} planes of Ni. The Ni peaks seemed broader due to its smaller grain size. Employing the MID Jade5.0 software, we calculated the grain size of the displaced Ni. The products from a concentration of  $2.34 \text{ g}\cdot\text{L}^{-1}$ ,  $1.17 \text{ g}\cdot\text{L}^{-1}$ , and  $0.78 \text{ g}\cdot\text{L}^{-1}$  had grain sizes of 2.1, 6.0, and 9.2 nm respectively. A reciprocal relationship between the grain size and the precursor concentration is inferred. During the typical course of heterogeneous nucleation, the deposition rate of tiny particles multiplies with increase of salt concentration<sup>[24]</sup>. However, if the salt concentration was too high, part of the  $\text{Ni}^{2+}$  ions could be hydrolyzed and form deposits. Therefore, the proper salt concentration is  $1.17 \text{ g}\cdot\text{L}^{-1}$ .



**Figure 3 :** XRD patterns of the Al/Ni prepared at different concentrations of  $\text{NiCl}_2\cdot 6\text{H}_2\text{O}$ : (a) raw Al; (b) concentration of  $2.34 \text{ g}\cdot\text{L}^{-1}$ ; (c) concentration of  $1.17 \text{ g}\cdot\text{L}^{-1}$ ; (d) concentration of  $0.78 \text{ g}\cdot\text{L}^{-1}$ .

### Corrosion characteristics of Al/Ni

After being ultrasonicated in distilled water, the as-

prepared Al/Ni nanocomposite particles were etched by a hydrochloric acid solution and a NaOH alkaline solution. When there were no bubbles rose, the etched residues were separated. The XRD patterns and SEM images of the residues are illustrated in Figure 4 and 5. The XRD patterns indicate that the Al core was approximately completely removed. In Figure 5a, after etched by acid, the Ni nanoshells remained. However, in an alkaline solution (as seen in Figure 5b), Ni shells broke into fragments as Al cores dissolved. In fact, no distinct concentration difference was observed between two solution (the hydrochloric acid solution had approximately 30 wt% HCl and the alkaline solution with a concentration of  $8 \text{ mol}\cdot\text{L}^{-1}$ ).

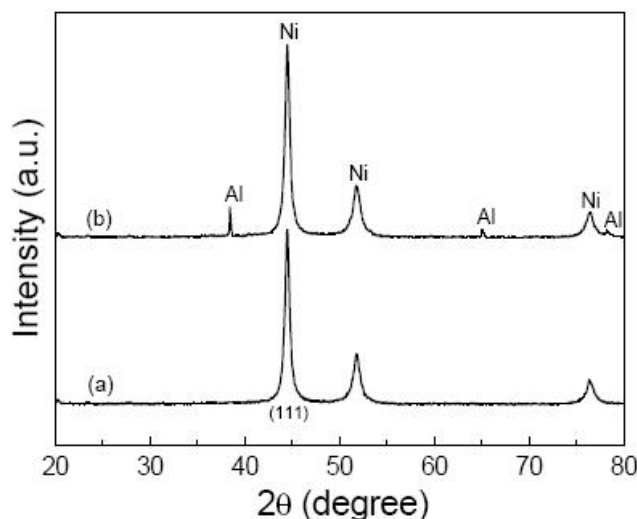


**Figure 4 :** XRD patterns of the etched residues: (a) Ni shells etched by hydrochloric acid; (b) Ni fragments etched by alkaline NaOH.

The experimental results suggested different etching mechanisms in acidic and alkaline solutions. In an acidic solution, the corrosion of Al particles initiated at the exposed Al surfaces further progress by penetrating (as schematized in Figure 6a and b). This indicates that etching may proceed outward in acids (Figure 6c and d). Finally, Ni shells imaged in Figure 5(a) were retained. In an alkaline solution, the corrosion of Al began at the surface and proceeded around the core surface without penetrating into the core (as schematized in Figure 6e and f). The furious effervescence at the beginning of the reaction made the shells broken into fragments (as shown in Figures 6g and h), which consists with the images in Figure 5b.

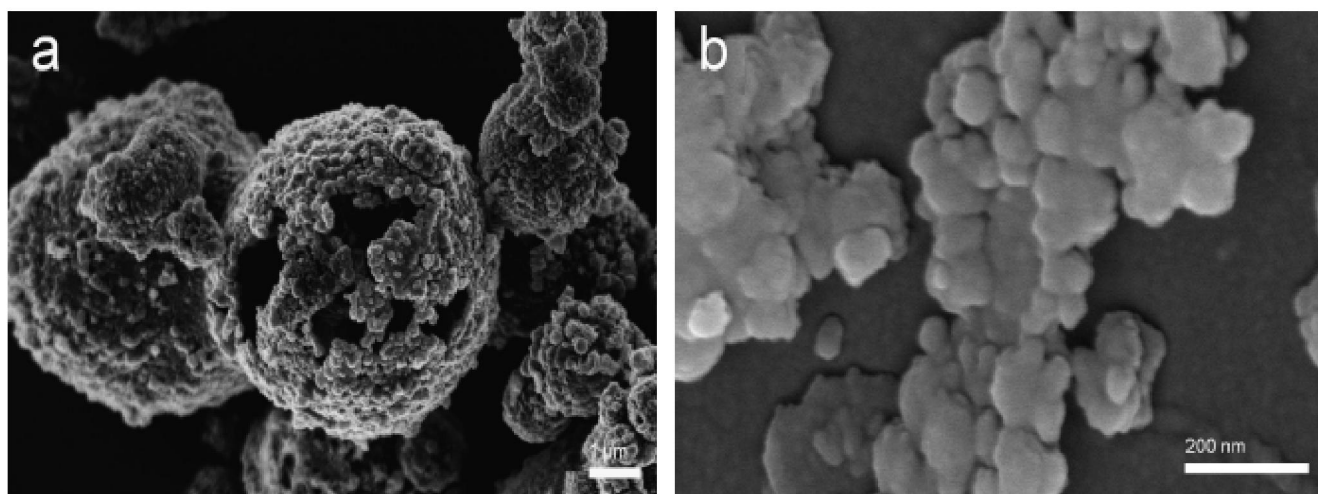


Figure : 5 SEM images of the etched residues: (a) Ni shells etched by hydrochloric acid; (b) Ni fragments etched by NaOH solution.

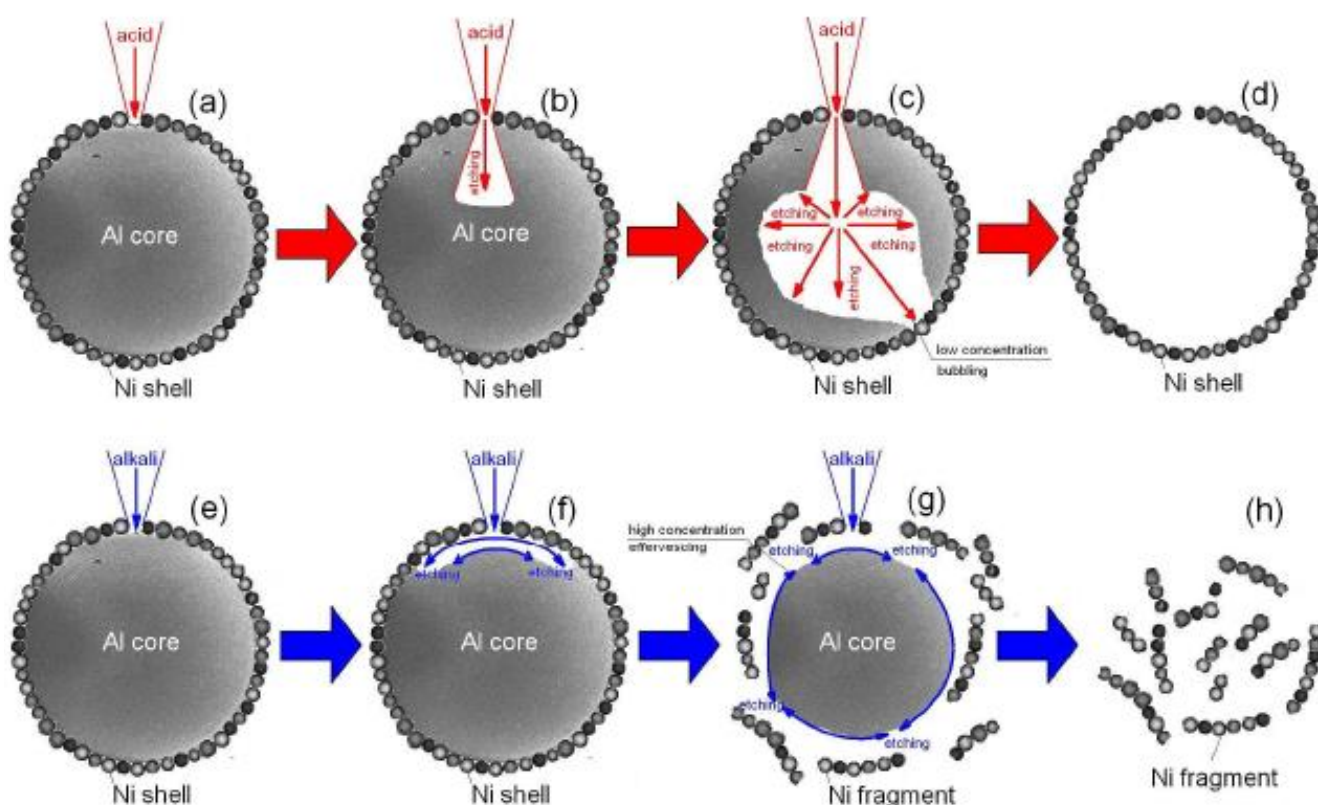


Figure : 6 Schematic diagrams of possible etching mechanisms for Al/Ni in hydrochloric acid (a-d) and NaOH solution (e-h).

## CONCLUSIONS

In this study, the displacement reaction between metallic Al and  $\text{Ni}^{2+}$  ions was employed to deposit Ni nanoparticles on micron Al *in situ*. In fabrication,  $\text{NH}_4\text{F}$  is the key to incur the redox reaction between  $\text{Ni}^{2+}$  and

Al, because it redounded to dissolve the alumina layers that blocked the displacement reaction. Several factors, such as surfactant,  $\text{NH}_4\text{F}$  concentration, and  $\text{NiCl}_2 \cdot \text{H}_2\text{O}$  concentration, were discussed. The  $\text{NH}_4\text{F}$  concentration of  $0.2 \text{ mol} \cdot \text{L}^{-1}$  and the  $\text{NiCl}_2 \cdot 6\text{H}_2\text{O}$  concentration of  $1.17 \text{ g} \cdot \text{L}^{-1}$  were proper. The PEG600 used as the surfactant not only protected the available Al but

## Full Paper

also prevented the overgrowth of Ni particles.

To investigate the corrosion characteristics of the Al/Ni bimetallic nanocomposites, the as-prepared Al/Ni nanocomposites were etched by a hydrochloric acid solution and an alkaline NaOH solution. The etched residues exhibited different morphologies. In acidic solution, the Al cores were dissolved while the Ni nanoparticles remained as hollow shells. In the alkaline solution, the metallic Al cores were also removed. However, the Ni shells were broken into fragments. Therefore, the mechanisms of acid etching and alkaline etching were outward and inward respectively.

### REFERENCES

- [1] K.M.Kang, H.W.Kim, I.W.Shim; *Fuel Process. Technol.*, **92**, 1236 (2011).
- [2] N.C.Zhang, Y.H.Gao, H.Zhang; *Colloids Surf. B:Biointerfaces*, **81**, 537 (2010).
- [3] Y.Chen, J.X.Lu, Z.G.Chen; *J.Inorg.Mater.*, **27**, 66 (2011).
- [4] Y.H.Sun, M.Zhang, J.J.Yang; *J.Inorg.Mater.*, **25**, 1965 (2009).
- [5] X.L.Zhong, K.L.Huang, S.Q.Liu; *J.Inorg.Mater.*, **25**, 19 (2009).
- [6] Y.Q.Kang, M.S.Cao, X.L.Shi; *Surf.Coatings*, **201**, 7201 (2007).
- [7] Z.F.Bian, J.Ren, J.Zhu; *Appl.Catalysis B: Environmental*, **89**, 577 (2009).
- [8] A.Hahma, A.Gany, K.Palovuori; *Combust.Flame*, **145**, 464 (2006).
- [9] A.Dokhan, E.W.Price, J.M.Seitzman; *Proc. Combust.Inst.*, **29**, 2939 (2002).
- [10] M.H.Keshavarz; *Combust.Flame*, **142**, 303 (2005).
- [11] S.Mohan, L.Furet, E.L.Dreizin; *Combust.Flame*, **157**, 1356 (2010).
- [12] M.A.Trunov, M.Schoenitz, X.Y.Zhu; *Combust. Flame*, **140**, 310 (2005).
- [13] Z.P.Cheng, Y.Yang, F.S.Li; *Trans.Nonferrous Metals Soc.China*, **8**, 378 (2008).
- [14] Y.Yang, Y.Z.Liu, F.S.Li; *J.Chem.Indust.Eng.China*, **156**, 2228 (2005).
- [15] Y.S.Kwon, A.A.Gromov, J.I.Strokova; *Appl. Surf.Sci.*, **253**, 5558 (2007).
- [16] X.D.Liu, Y.Yang, F.S.Li; *Functional Mater.*, **37**, 1135 (2006).
- [17] X.D.Xiong, Y.W.Tian, X.J.Zhai; *Chinese J. Nonferrous Metals*, **6**, 39 (1996).
- [18] X.D.Xiong, Y.C.Zhai, Y.W.Tian; *J.Northeastern Univ.*, **17**, 512 (1996).
- [19] G.J.Mou, B.Zhao; *Chinese J.Inorg.Chem.*, **20**, 1055 (2004).
- [20] Z.J.Liu, B.Zhao, Z.T.Zhang; *Chinese J.Inorg. Chem.*, **12**, 30 (1996).
- [21] B.J.Gao, H.M.Jiang, Z.X.Zhang; *Chinese J.Inorg. Chem.*, **16**, 669 (2000).
- [22] R.H.Perry, D.W.Green; 'Perry's chemical engineers handbook, Sci.Press; Beijing, (2001).
- [23] Y.Zhang, D.P.Li, L.Yang; *Chin.J.Analytical Chem.*, **33**, 974 (2005).
- [24] F.S.Li; 'Technology and application of nano/micron composing', National Defence Industrial Press; Beijing, (2002).